



SEISMIC QUALIFICATION AND FRAGILITY TESTING OF SUSPENDED CEILING SYSTEMS

Hiram BADILLO-ALMARAZ¹, Andrew S. WHITTAKER² and Andrei M. REINHORN³

SUMMARY

The failure of suspended ceiling systems (SCS) has been one of the most widely reported types of nonstructural damage in past earthquakes. Fragility methods were used in this study to characterize the vulnerability of SCS. Since SCS are not amenable to traditional structural analysis, full-scale experimental testing on an earthquake simulator was performed to obtain fragility data. Several ceiling-system configurations were studied. The results from the full-scale testing are presented in form of seismic fragility curves. Four limit states of response that cover most of the performance levels described in the codes and guidelines for the seismic performance of nonstructural components were defined using physical definitions of damage. Data was obtained for every limit state to compare the effect of each configuration on the response of the SCS. Based on the results of the experimental testing it was found that (a) the use of retainer clips generally improved the performance of SCS, (b) undersized (poorly fitting) tiles are substantially more vulnerable than properly fitted tiles, (c) including recycled cross-tees in the assemblage of the suspended grid increased the vulnerability of the SCS, and (d) including compression posts improves the seismic performance in SCS.

INTRODUCTION

The response of nonstructural components can significantly affect the functionality of a building after an earthquake, even when the structural components are undamaged. Poor performance of nonstructural components in past earthquakes has led to the evacuation of buildings, substantial economic losses due to business interruption and in extreme cases to the loss of life. The failure of SCS has been one of the most widely reported types of nonstructural damage in past earthquakes. Reconnaissance has shown that failures of SCS during earthquakes have caused significant economic losses and disruption in important or critical facilities.

¹ Graduate Student, Department of Civil, Structural, and Environmental Engineering, State University of New York at Buffalo, 212 Ketter Hall, Buffalo, NY 14260. Email: hb5@eng.buffalo.edu

² Associate Professor, Department of Civil, Structural, and Environmental Engineering, State University of New York at Buffalo, 230 Ketter Hall, Buffalo, NY 14260. Email: awhittak@eng.buffalo.edu

³ Clifford C. Furnas Professor, Department of Civil, Structural, and Environmental Engineering, State University of New York at Buffalo, 231 Ketter Hall, Buffalo, NY 14260. Email: reinhorn@buffalo.edu

Earthquake-history testing has been used recently for qualification and fragility testing of structural and nonstructural components. Seismic qualification is intended to demonstrate through experimentation that a component in a structure is able to function during and after an earthquake. In contrast to qualification testing, the objective of fragility testing is to establish a relationship between limit states of response and a representative excitation parameter for a component. The development of fragility curves generally involves the use of both mathematical modeling and physical observations. In the case of SCS, mathematical analysis is difficult to accomplish due to uncertainties in the physical behavior of elements and components of the system once that they are installed in the ceiling system. Further, the complexity of the mathematical model and the highly nonlinear behavior of the components once tiles are dislodged make robust structural analysis of SCS virtually impossible. Since analytical methods are generally not applicable to the study of SCS and data collected following past earthquakes are not suitable for fragility characterization, experimental methods represent the best and most reliable technique to obtain fragility curves for SCS.

The main goal of this study was to develop fragility curves of SCS subjected to earthquake shaking. Fragility curves were obtained by experimental testing of SCS on an earthquake simulator. The specific objectives of the research program were: (1) to study the performance of a SCS that is commonly installed in the United States; (2) to evaluate improvements in response offered by the use of retainer clips that secure the ceiling panels (tiles) to a suspension system; (3) to investigate the effectiveness of including a vertical strut (or compression post) as seismic reinforcement in ceiling systems; and (4) to evaluate the effect of different boundary conditions on the response of a SCS.

SEISMIC FRAGILITY AND PREVIOUS STUDIES ON SUSPENDED CEILING SYSTEMS

Seismic fragility has been defined as the conditional probability of failure of a system for a given intensity of a ground motion. In performance based seismic design, failure is said to have occurred when the structure fails to satisfy the requirements of a prescribed performance level. If the intensity of the ground motion is expressed as a single variable (e.g., the peak ground acceleration or the mapped maximum earthquake spectral acceleration at short periods, etc.), the conditional probability of failure expressed as a function of the ground motion intensity is called a seismic fragility curve (Sasani and Der Kiureghian [1]). Fragility curves can be generated via testing or numerical analysis.

Although several studies have indicated that some improvement in the seismic capacity of SCS has been achieved in recent years (Rihal and Granneman [2], ANCO [3], and Yao [4]), there exists no robust fragility data for SCS and no proven strategies to increase the seismic strength of SCS. From 2001 through 2003, Armstrong World Industries Inc. undertook an extensive series of earthquake qualification tests on SCS at the University at Buffalo (Badillo [5] and Badillo et al. [6]). The fragility studies described below build on these qualification studies.

EXPERIMENTAL FACILITIES FOR SEISMIC TESTING AND TEST SPECIMENS

Earthquake Simulator and Test Frame

The earthquake simulator in the Structural Engineering and Earthquake Simulation Laboratory (SEESL) of the State University of New York at Buffalo was used to evaluate and qualify the ceiling systems. The performance envelope of the table is ± 152 mm (6 in.) displacement, ± 762 mm/sec (30 in./sec) velocity and 1.15g acceleration at a payload of 197 kN (44 kips) in the horizontal direction, and ± 76 mm (3 in.) displacement, ± 508 mm/sec (20 in./sec) velocity, and 2.30g acceleration in the vertical direction.

A 4.88 x 4.88 m (16 x 16 ft) square frame of ASTM Grade 50 steel was constructed to test the ceiling systems. The frame was attached to the simulator platform using 25 mm (1 in.) diameter bolts in the

beams that were oriented in the East-West direction. Two 10.2 x 10.2 cm (4 x 4 in.) tubular sections connected at each corner served as main columns of the frame. A 3.8 x 3.8 cm (1-1/2 x 1-1/2 in.) angle was welded around the perimeter of the test frame. A 5.1 x 15.2 cm (2 x 6 in.) timber ledger was attached to the angle. The perimeter timber ledger served as a *stud wall* and anchored the ceiling system. For a detailed description of the features of the test frame refer to Badillo [5] and Badillo et al. [6]. Figure 1 is a photograph of the test frame mounted on the earthquake simulator at the University at Buffalo.

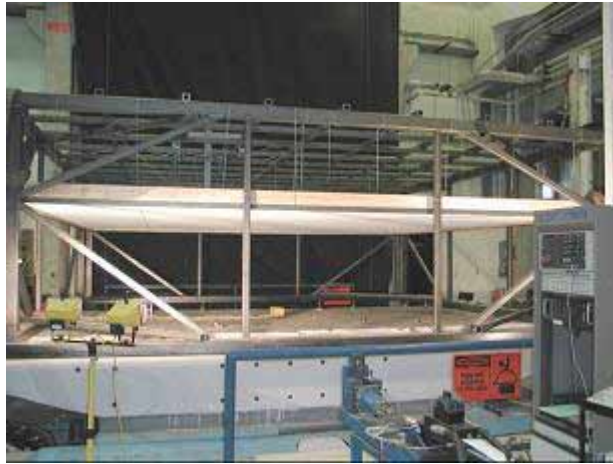


Figure 1. Test frame mounted on the simulator at the University at Buffalo

Specimen Description

Each ceiling system consisted of two key components: a suspension system and tiles. In some configurations retention clips were added to the ceiling systems. All components used in this study were off-the-shelf items used in commercial ceiling construction. Accelerometers and displacement transducers were used to monitor the response of the simulator platform, the test frame and the ceiling support grid.

Suspension Grid

The ceiling systems were installed in a grid that was hung with suspension wires from the top of the test frame. The grid was constructed with a 23.8 mm (15/16 in.) exposed tee system. A 5.1-cm (2-in.) wall molding was attached to the perimeter timber ledger. The main runners and cross runners were attached to the wall molding with rivets on the South and West sides of the frame, while the runners on the North and East sides floated free. The main runners were installed in the North-South direction at spacing of 1.22 m (48 in.) on center. The 1.22 m (4 ft) cross runners were installed in the East-West direction at spacing of 61 cm (24 in.) on center, whereas the 61cm (2 ft) cross runners were installed in the North-South directions at a spacing of 1.22 m (48 in.) on center. A compression post was placed 1.52 m (5 ft) from the South and the East sides of the frame.

Tiles

Since the actual sizes of ceiling tiles may differ from the nominal size depending on quality control used in the manufacturing process, two types of tiles were used for fragility testing in this study. Based on personal communications with practicing engineers and manufacturers, ceiling tiles were considered to be of *normal size* if their plan dimensions are not smaller than the nominal dimensions by more than 6.4 mm (1/4 in.) and *undersized* otherwise. One of the tiles tested was a Fine Fissured Humigard Plus tile. This tile was smaller than the nominal size by at least 12.7 mm (1/2 in.) and was therefore considered to be an undersized tile. The other tile used in this study was the Humigard Plus tile. This tile was a normal sized tile. Table 1 presents summary information on each of the two tiles used in this study. A total of 49 tiles

were installed in the inner seven rows (seven tiles in each row). Cut tiles were used in the perimeter rows of the ceiling system. Figure 2 is a photograph of the Humigard Plus tile.

TABLE 1. Summary information on the tiles used in this study

<i>Tile Name</i>	<i>Description</i>	<i>Panel dimensions [B, D, T] *</i>		<i>Weight (kg/tile)</i>
		<i>Nominal Size (cm)</i>	<i>Actual Size (cm)</i>	
Fine Fissured Humigard Plus	Mineral fiber tile	61 x 61 x 1.6	59.7 x 59.7 x 1.6	1.3
Humigard Plus	Mineral fiber tile	61 x 61 x 1.6	60.3 x 60.3 x 1.6	1.7

* *B*, *D* and *T*: breadth, depth and thickness, respectively

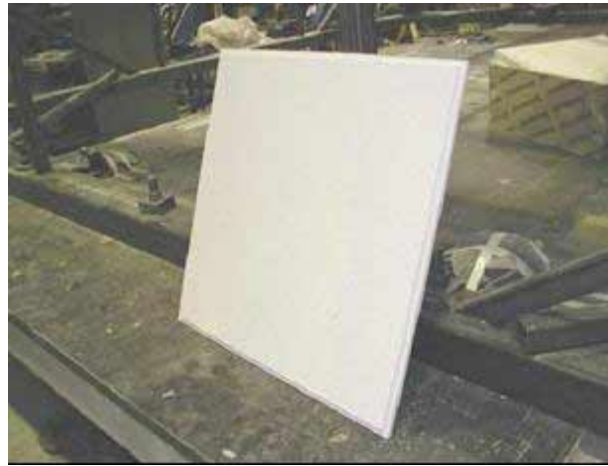


Figure 2. Humigard Plus ceiling tile

Clips

Clips similar to those shown in Figure 3 were installed to investigate possible improvements in the seismic performance of SCS. These clips can be attached to main beams or cross tees behind lay-in ceiling tiles and help to prevent the panes from dislodging. In this study, the clips were installed on the 1.22 m (4 ft) long cross tees of the grid.

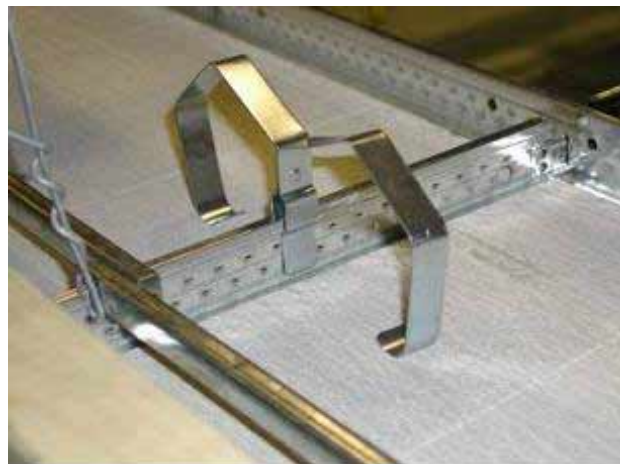


Figure 3. Retention clips

DYNAMIC CHARACTERISTICS OF THE TEST FRAME

The test frame was designed to represent in an approximate sense the horizontal and vertical stiffness of a story in a building structure. The dynamic characteristics of the test frame were evaluated along the two programmable axes of the earthquake-simulator platform, namely, the North-South and vertical directions. Three methods were used to identify the dynamic properties of the test frame: free vibration, by means of a snap-back test, and two forced vibration tests, by means of resonance search and white noise tests. Details are provided in Badillo [5] and Badillo et al. [6]. The horizontal and vertical frequencies of the frame were 12 and 10 Hz, respectively. The damping ratios in the fundamental horizontal and vertical modes were approximately 3% and 0.5%, respectively.

SEISMIC QUALIFICATION AND FRAGILITY TESTING PROTOCOL

Testing Protocol

The testing protocol for fragility testing consisted of sets of horizontal and vertical dynamic excitations. Each set included unidirectional and bi-directional resonance search tests using white noise excitation along each programmable orthogonal axis of the simulation platform (North-South and vertical). Each set of excitations also included a series of unidirectional and bi-directional spectrum-compatible earthquake motions that were established for different multiples of ICBO-AC156 Required Response Spectrum (Badillo [5], Badillo et al. [6] and ICBO [7]). The parameter selected to characterize the ground motion for input to the simulator was the mapped spectral acceleration at short periods, S_S (ICC [8]). The target levels for earthquake simulation ranged from a $S_S = 0.25$ g through $S_S = 2.5$ g. Information on the generation of the earthquake histories for testing is presented in Badillo [5] and Badillo et al. [6]. Figure 4 presents the horizontal and vertical RRS and their corresponding response spectra calculated from records generated for a level of shaking corresponding to $S_S = 1.0$ g.

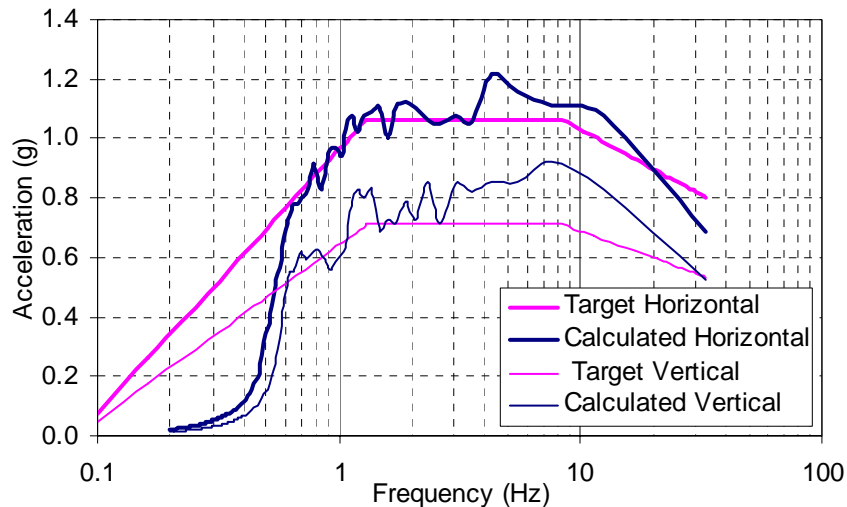


Figure 4. Horizontal and vertical response spectra (target and calculated) for a level of shaking corresponding to $S_S = 1.0$ g.

RESULTS OF SIMULATOR TESTING

Four variables that affect the seismic performance of SCS were investigated in this study: (a) the size and weight of tiles, (b) the use of retainer clips, (c) the use of compression posts, and (d) the physical condition of grid components. Information on variables (a) and (b) are presented in this paper; results for variables (c) and (d) can be found in Badillo [5] and Badillo et al. [6]. A total of six set-ups were

configured using different combinations of these variables: (1) undersized tiles (series A-D), (2) undersized tiles with retainer clips (series E-G), (3) normal sized tiles (series L-O, Q, R and BB), (4) normal sized tiles with retainer clips (series P and S-U), (5) normal sized tiles without the compression post (series: V-Z and AA) and (6) undersized tiles with recycled grid components (series H-J). Summary test information on configurations (1) through (4) is presented below.

Configuration 1: Undersized Tiles

The undersized tiles failed typically by first popping up out of the suspension grid and then falling through the grid to the simulator platform below. Figure 5 shows a tile an instant before it fell to the earthquake simulator below.



Figure 5. Tile rotating before falling, configuration 1

Configuration 2: Undersized Tiles with Retainer Clips

The retainer clips substantially improved the behavior of the SCS in terms of loss of tiles by comparison with the systems of configuration 1. By retaining the tiles, the clips increased the inertial loads on the grid, resulting in grid damage at lower levels of shaking. Figure 6 shows a buckled 1.22 m (4-ft) cross tee following severe earthquake shaking. Another type of commonly observed damage to the grid components was failure and fracture of the latches of the cross tees. In the systems of configuration 2, tiles were lost primarily due to failure of grid components.



Figure 6. Buckling in 4-ft cross tees, configuration 2

Configuration 3: Normal Sized Tiles

The number of tiles that fell during the simulator tests of ceiling systems with undersized or poorly fitting tiles was substantially larger by comparison with the systems equipped with normal sized (snug) tiles. However, ceiling system performance in terms of damage to grid components was better in the systems with undersized tiles because the weight of the normal sized tiles was larger (1.7 kg/tile) than the undersized tiles (1.3 kg/tile), and the number of tiles that stayed in place during shaking was larger for the systems of configuration 3, and therefore the inertial loads on the suspension grid were larger for configuration 3 than in configuration 1. The buckling in the web of the 1.22 m (4-ft) cross tees was similar to the damage that the grid components experienced in configuration 2 during higher levels of shaking. The tile failure pattern in configuration 3 was similar to that of configuration 1.

Configuration 4: Normal Sized Tiles with Retainer Clips

The retainer clips substantially improved the behavior of the SCS in terms of loss of tiles by comparison with the systems of configuration 3, where clips were not included. The use of the retainer clips shifted the damage from the tiles to the suspension grid. The type of damage that was observed in the 1.22 m (4-ft) cross tees of configuration 2 was also observed in the systems of configuration 4. In both systems, the loss of tiles was primarily due to the failure of grid components.

FRAGILITY ANALYSIS AND DATA EVALUATION

One of the purposes of fragility analysis is to identify the seismic vulnerability of systems (or components of a system) associated with various states of damage. A fragility curve describes the probability of reaching or exceeding a damage (or limit) state at a specified level of excitation. Thus, a fragility curve for a particular limit state is obtained by computing the conditional probabilities of reaching or exceeding that limit state at various levels of excitation. A plot of the computed conditional probabilities versus the ground motion parameter describes the fragility curve for that damage state (Singhal and Kiremidjian [9]). The conditional probability of reaching or exceeding a damage state is:

$$P_{ik} = P[D \geq d_i | Y = y_k] \quad (4)$$

where P_{ik} is the probability of reaching or exceeding a damage state d_i given that the excitation is y_k ; D is a damage random variable defined on damage state vector $\mathbf{D} = \{d_0, d_1, \dots, d_n\}$; and Y is an excitation random variable.

Limit States

Four limit states were defined in this study to characterize the seismic response of SCS. Limit states 1 through 3 account for the number (or percentage) of tiles that fell from the suspension grid. The fourth limit state is associated with structural damage to the suspension grid. The four limit states were: (1) minor damage (loss of 1% of the tiles from the grid), (2) moderate damage (loss of 10% of the tiles from the grid), (3) major damage (loss of 33% of the tiles from the grid), and (4) grid failure. Detailed descriptions of these limit states are provided in Badillo [5] and Badillo et al. [6].

Ground Motion Intensity Parameters

Several intensity parameters have been used in previous studies to create fragility curves, namely peak ground acceleration, peak ground velocity, spectral acceleration at specific periods, and spectral acceleration over a frequency range that would bracket the in-service dynamic properties of a specific system. There is no uniformly accepted intensity measure for a use in the construction of fragility curves.

In this study, two excitation parameters were used to construct the fragility curves presented below and in Badillo [5] and Badillo et al. [6]: (1) peak ground acceleration, and (2) average horizontal spectral

accelerations at selected periods. The selected periods represent a broad range that should include most in-service conditions for SCS in buildings: 0.2, 0.5, 1.0, 1.5 and 2.0 seconds. The spectral acceleration ordinates were obtained by calculating the mean spectral acceleration for each ceiling system configuration tested at each level of earthquake shaking.

Evaluation of Fragility Data

The four limit states used to characterize the seismic performance of SCS were selected with the intent of covering most of the performance levels described in current seismic codes and guidelines for seismic performance of nonstructural components. The procedure to develop the fragility curves for each configuration is illustrated in Figure 7. The data presented in the illustration of the procedure is from the 6 systems that were part of configuration 3: Systems L, M, N, O, R and BB. The procedure was as follows: (1) obtain the mean spectral acceleration response for each shaking level with the accelerometer mounted on the simulator platform (see the heavy solid line in Figure 7), (2) compute the spectral accelerations at selected periods (0.2, 0.5, 1.0, 1.5 and 2.0 seconds) from the mean spectral accelerations (see the arrows in Figure 7 for the 1-second calculation, $S_{1.0} = 2.36$ g), (3) count the number of tiles that fell from the grid for each system (6 systems in this example) at each shaking level as a percentage of the total number of tiles in the ceiling system, (4) compare the percent tile failure with each limit state for each system, and (5) calculate the probability of reaching or exceeding the limit state as:

$$P_f = \frac{N_f}{N} \quad (5)$$

where N_f is the number of systems (trials) where the limit state was reached or exceeded and N is the total number of systems in configuration. As N approaches infinity, P_f approaches the true probability of reaching or exceeding a limit state. The fragility curves were obtained by plotting P_f for each shaking level versus the corresponding mean spectral acceleration. The process was repeated for each of the six configurations tested in this study.

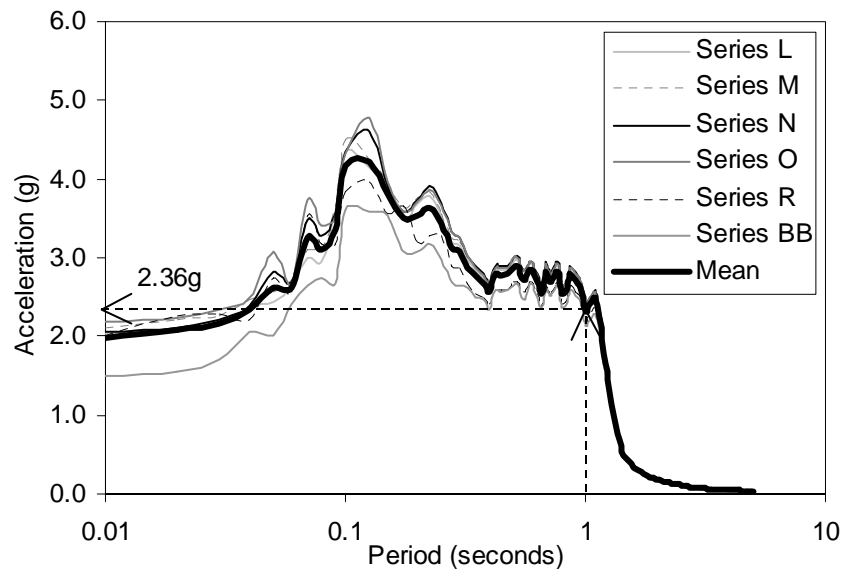
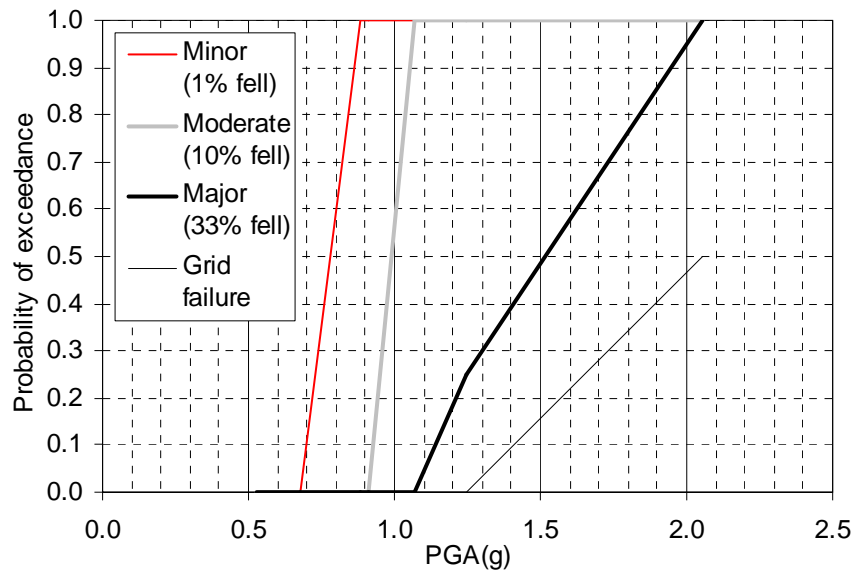


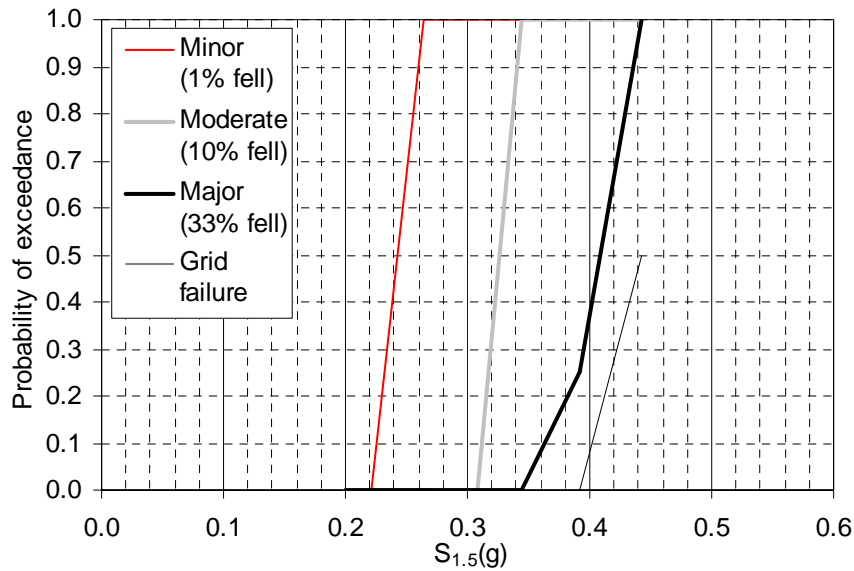
Figure 7. Procedure to develop fragility curves, configuration 3: normal sized tiles

Figure 8a presents the fragility curve for peak ground acceleration (0 second period spectral acceleration) and Figure 8b presents the fragility curve for the spectral period of 1.5 seconds, for configuration 1 for

each limit state defined earlier. Similar figures were obtained in this study for each of the spectral acceleration periods selected and for each of the six configurations.



a) Fragility curves for peak ground acceleration

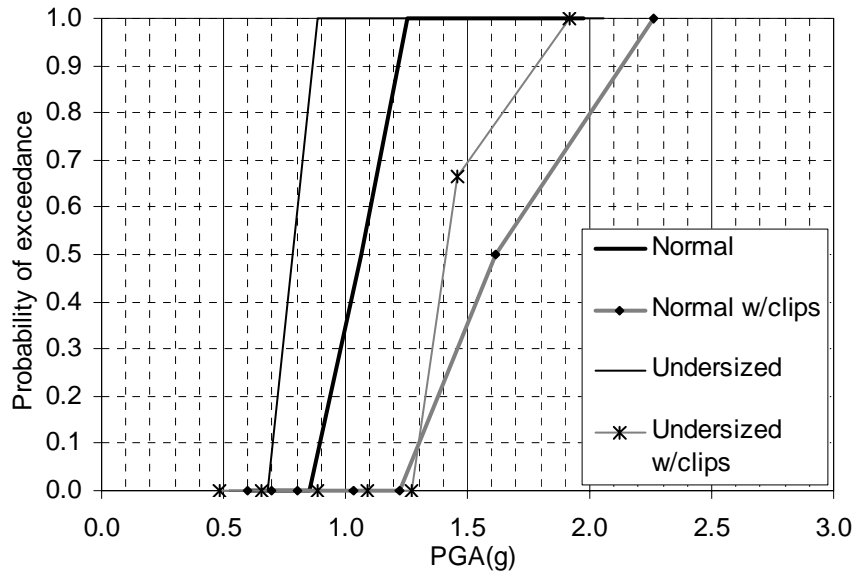


b) Fragility curves for spectral acceleration at 1.5 seconds

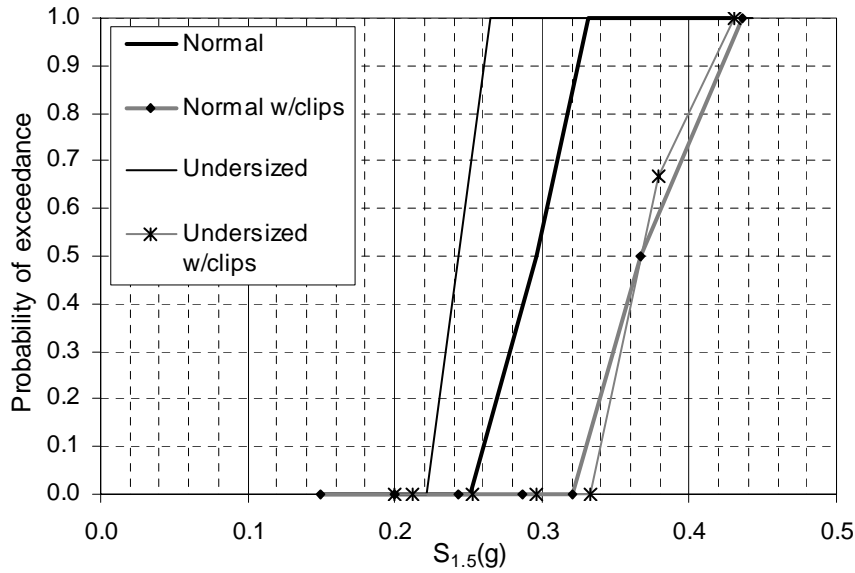
Figure 8. Fragility curves for configuration 1: undersized tiles

Figure 9 presents the same information presented in Figure 8 but for the first four of the six configurations tested in this study for the case of minor damage. Similar figures were obtained in this study for each of the spectral acceleration periods selected and for each limit states defined. Some of the fragility curves were incomplete because the maximum acceleration, velocity, and displacement of the simulator are limited to 1.5g, 94 cm/sec (37 in/sec) and 14 cm (5.5 in.), respectively. Different scales were used in

plotting the fragility curves because the magnitude of the spectral acceleration changed substantially as a function of period.



a) Fragility curves for peak ground acceleration



b) Fragility curves for spectral acceleration at 1.5 seconds

Figure 9. Fragility curves for limit state 1: minor damage

CONCLUSIONS

1. The most common failure mode of tiles when retention clips were not used was tiles popping out of the grid. If the tiles did not return to the original position on the suspension system, it was very likely for the tiles to rotate and fall to the simulator platform below.

2. The use of retainer clips substantially improved the behavior of the SCS in terms of loss of tiles. However, by retaining the tiles, the use of clips increased the inertial loads on the grid, resulting in grid damage at lower levels of shaking. The loss of tiles in systems with retention clips was due primarily to the failure of grid components.
3. The effect of a small variation in tile size on the performance of the SCS was considerable in terms of loss of tiles. Even when the weight of normal sized tiles was larger than the weight of the undersized tiles by a 30% approximately, the number of tiles that fell during the shaking tests of ceiling systems with undersized tiles was substantially larger by comparison with the systems equipped with normal sized tiles. However, ceiling system performance in terms of damage to grid components was better in the systems with undersized tiles because the inertial loads on the suspension grid were smaller than in those systems with normal sized tiles.
4. The rivets that attached the main runners and cross tees to the wall molding played a very important role in the seismic performance of the SCS. Damage in the ceiling systems in terms of loss of tiles was much larger when a rivet failed than when all of the rivets were undamaged and the cross tees remained firmly attached to the wall molding.
5. Presenting information in the form of fragility curves appears to be a convenient way to represent the seismic behavior of SCS. Fragility curves help to identify regions of undesirable and unsafe performance of SCS, such as the case when two fragility curves intersect. For example, the region beyond the intersection of fragility curves for limit state 3 (major tile failure) and limit state 4 (grid failure) should be avoided because failure of large sections of tiles and grid could cause a life-safety hazard.

ACKNOWLEDGMENTS

Armstrong World Industries Inc. provided all of the ceiling system components for the fragility testing program. This support is gratefully acknowledged. Special thanks are due to Messrs Paul Hough and Thomas Fritz of Armstrong World Industries and Messrs Mark Pitman, Scot Weinreber and Dwayne Kowalski of the Department of Civil, Structural and Environmental Engineering at University at Buffalo.

The first author would like to thank to the National Council of Science and Technology of Mexico (CONACYT) for their financial support during his stay at the State University of New York at Buffalo. Partial support for the work described in this paper was provided by the Multidisciplinary Center for Earthquake Engineering Research through grants from the Earthquake Engineering Centers Program of the National Science Foundation (Award Number EEC-9701471) and the State of New York.

REFERENCES

1. Sasani, M. and Der Kiureghian, A. "Seismic Fragility of RC Structural Walls: Displacement Approach", *Journal of Structural Engineering* 2001; 127(2): 219-228.
2. Rihal, S., and Granneman, G. "Experimental Investigation of the Dynamic Behavior of Building Partitions and Suspended Ceilings During Earthquakes", Rep. No. ARCE R84-1, California Polytechnic State University, Pomona, California, 1984.
3. ANCO. "Earthquake Testing of a Suspended Ceiling System", ANCO Inc., Culver City, Cal., 1993.
4. Yao, G. C. "Seismic Performance of Direct Hung Suspended Ceiling Systems", *Journal of Architectural Engineering* 2000; 6(1): 6-11.
5. Badillo, H. "Seismic Fragility Testing of Suspended Ceiling Systems", M.S. Thesis, School of Engineering, State University of New York at Buffalo, Buffalo, New York, 2003.
6. Badillo, H., Whittaker, A. S., and Reinhorn, A. M. "Seismic Fragility of Suspended Ceiling Systems", Paper to be submitted for possible publication, *Earthquake Spectra*, March 2004.

7. ICBO “ICBO AC156 Acceptance Criteria for the Seismic Qualification of Nonstructural Components”, ICBO Evaluation Service, Whittier, California, 2000. 90601-2298.
8. ICC. “International Building Code”, International Code Council, Falls Church, Virginia, 2000.
9. Singhal, A. and Kiremidjian, A. S. “Method for Probabilistic Evaluation of Seismic Structural Damage”, *Journal of Structural Engineering* 1996; 122(12): 1459-1467.
10. Shinozuka, M., Feng, M. Q., Lee, J., and Naganuma, T. “Statistical Analysis of Fragility Curves”, *Journal of Engineering Mechanics* 2000; 126(12): 1224–1231.